ELSEVIER

Journal of Nuclear Materials 290–293 (2001) 783–787

journal of nuclear materials

www.elsevier.nl/locate/jnucmat

Modeling of carbon transport in the divertor and SOL of DIII-D during high performance plasma operation

W.P. West [a,*], G.D. Porter [b], T.E. Evans [a], P. Stangeby [c], N.H. Brooks [a], M.E. Fenstermacher [b], R.C. Isler [d], T.D. Rognlien [b], M.R. Wade [d], D.G. Whyte [e], N.S. Wolf [b]

[a] *General Atomics, P.O. Box 85608, San Diego, CA 92186-5608, USA*
[b] *Lawrence Livermore National Laboratory, Livermore, CA, USA*
[c] *University of Toronto Institute for Aerospace Studies, 4925 Dufferin St, Toronto, Canada M3H 5T6*
[d] *Oak Ridge National Laboratory, Oak Ridge, TN, USA*
[e] *University of California, San Diego, CA, USA*

Abstract

The UEDGE modeling code has been used to study the effect of varying the carbon yield from the plasma facing surfaces on the core plasma carbon contamination in DIII-D. The model of the lower single-null, ELMing H-mode plasma shows a remarkably weak dependence of the core carbon concentration over an approximate factor of two variation in the source. This weak dependence is in agreement with the analysis of spectroscopic data from DIII-D [1]. Examination of the carbon transport shows a general flow pattern of carbon as follows: (1) parallel flow from the divertors to the near scrape off layer (SOL) near the separatrix, (2) cross field diffusion from the near SOL to the far SOL (near the wall), and (3) parallel flow from the far SOL to the far region of the inner divertor. The carbon flux from the divertors to the near SOL drops as the sputtering rate is reduced. In the far SOL, background plasma parameters adjust in small ways to produce an increasing carbon density with decreasing sputtering yield. This increasing density of carbon in the far SOL is consistent with a reduction in the parallel velocity of carbon ions flowing from the far SOL back to the inner divertor. Since the carbon density near the separatrix is constant as the sputtering yield is reduced, the increasing density in the far SOL reduces the radial gradient and therefore the diffusive radial flow. A balance in the outward radial diffusive flow from the near SOL and the flow from the divertor into the near SOL maintains the carbon density in the near SOL nearly constant, even though the carbon throughput changes. © 2001 Published by Elsevier Science B.V.

Keywords: Impurity transport; Impurity source; Fluid modeling; Carbon; DIII-D

1. Introduction

This study is motivated by a recent survey of spectroscopic data from DIII-D [1] showing a decrease in divertor carbon source by a factor of three to four over the past several years, but little change in typical core carbon concentration during ELMing H-mode operation. The need to provide the advanced tokamak program on DIII-D with control of impurities is also a strong motivator of this study. The advanced tokamak program demands operation at low plasma density ($n_e/n_{GW} < 0.5$), high plasma temperature, and low Z_{eff} in order to efficiently control the current profile and optimize performance ($\beta_N * \tau_E$). It is expected that the low-density, high-temperature plasmas will result in significant backflow of impurity ions along the divertor leg in the region near the separatrix. This results from the fact that the ion temperature gradient force that pulls impurity ions toward the midplane will increase significantly as the scrape off layer (SOL) ion temperatures just outboard of the midplane separatrix increase.

* Corresponding author. Tel.: +1-858 455 2863; fax: +1-858 455 3569.
E-mail address: west@fusion.gat.com (W.P. West).

0022-3115/01/$ - see front matter © 2001 Published by Elsevier Science B.V.
PII: S0022-3115(00)00535-3

At the same time, as the recycling flux decreases as density decreases, and as the divertor ion temperature increases somewhat, the frictional drag force that tends to keep impurity ions confined in the divertor decreases. Previous theoretical work has shown that strong impurity backflow can occur when the ion thermal gradient force dominates the frictional force from the primary ion flow [2–4]. The 2D modeling described here indicates that these low-density, high-performance plasmas result in such a condition. As shown clearly by Stangeby and Elder [2], such a backflow would lead to a catastrophically high carbon concentration were it not for radial transport to the far SOL. In these UEDGE results, transport of carbon in the far SOL is a major contributor to the lack of dependence of core carbon contamination on the sputtering yield.

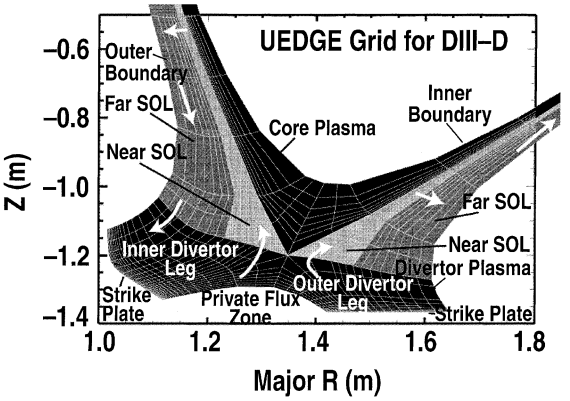

Fig. 1. Lower portion of the UEDGE grid. The core plasma and divertor plasma regions are filled in black. The near SOL region ($1.0 < \psi_{norm} < 1.01$) is filled in a light gray, and the far SOL ($\psi_{norm} > 1.015$) in a darker gray. The white arrows are illustrative of the general carbon flow pattern discussed in the paper.

2. The UEDGE model

The UEDGE code is a 2D multifluid model of the axisymmetric tokamak edge, SOL, and divertor plasma. It has been described in detail elsewhere [5,6]; we present only a brief description. A 2D non-orthogonal grid is produced using the EFIT MHD reconstruction of an actual DIII-D discharge [7]. Particle continuity and parallel momentum equations are solved for the deuterium ions and neutrals and for the impurity neutrals and each ionization state. Parallel transport is assumed to be classical [8], but flux limits are implemented to reduce anomalous effects of strong gradients. A Navier–Stokes fluid model [9] is used for the deuterium neutrals, and a diffusive model is used for the impurity neutrals. The impurity parallel momentum equation is a simple force balance [6]; inertial terms are ignored. Perpendicular transport is considered diffusive, with fuel and impurity ion diffusivities, and ion and electron thermal diffusivities were determined in previous work by comparison to data.

The UEDGE grid used in this study is shown in Fig. 1. The edge of the UEDGE domain is used as the wall or divertor plate location. The wall can be broken up into several sections. Multiple boundary conditions are available, but only those used in this study are described here. The recycling coefficient for ions returning from surfaces as neutrals is set to 1(0) for deuterium (impurity). The albedo at the side walls is 0.95(0) for deuterium (impurity) neutrals. At the divertor the plasma carries particles and energy to the plate along the B field at the ion-acoustic speed. As a consistency check, results are also presented for fixed impurity ion densities at the outer boundary. The power crossing the inner boundary for the ion and electron channels is set to match the experiment. The power into each cell along the inner boundary is distributed according to the local gradient of magnetic flux. No power is assumed to flow into the outer boundary.

The carbon sputtering yield within UEDGE is calculated based on the incident deuterium ion and neutral flux, the ion and electron temperatures, and the plate surface temperature. The Haasz/Davis [10] model is used for chemical sputtering, with a linear reduction of the sputtering yield for incident ion energies below 10 eV. The Eckstein model [11] is used for physical sputtering. To scan the carbon yield, we adjust a constant, Y_c, which multiplies the sputtering coefficient. Recycled and sputtered species are assumed to consist of only atomic neutrals, the presence of molecules is ignored. Self-sputtering by carbon ions is ignored. The deuterium and impurity neutrals can independently assigned to be at the local ion temperature, or assigned a fixed energy. In all cases presented here, the deuterium neutrals are at the local ion temperature, and the carbon neutrals are assigned a fixed energy of 2.5 eV (reasonably characteristic of carbon atoms from physical sputtering or from molecular breakup). The STRAHL rates for ionization, recombination, and radiation rates for carbon [12] are used in UEDGE.

3. UEDGE plasma solutions and carbon transport

A DIII-D ELMing H-mode plasma is used as a basis for this study, shot 94 002 at 1750 ms. This LSN plasma was heated by 8 MW of injected neutral deuterium beams. Most of the basic input parameters are shown in Table 1. The initial input parameters are based on a previous UEDGE study of this discharge. This modeling effort is not intended to match in detail a particular

Table 1
UEDGE input parameters used in this study

Inner boundary	Power flow, electrons: 4.0 MW, ions: 4.0 MW Deuterium ion density: 3.35×10^{19} m^{-3}
Transport	Particle diffusivity: 0.1 m^2/s (all ion species)
Thermal diffusivities	Ion: 0.36 m^2/s, electron: 0.36 m^2/s
Sputtering yield multiplier	Scanned from 0.4 to 1.4

DIII-D plasma, but is intended as an investigation of a single parametric scan, that is the sputtering multiplier, Y_c. Because of the inherent coupling of the impurities in the UEDGE multifluid model, the basic plasma parameters do change as the carbon influx is changed; however in this case, the only large change occurred at the outer strike plate. Tables 2 and 3 show the range of variations of a few important parameters from the UEDGE solutions. Key features are: (1) an attached outer divertor leg, (2) a detached inner leg, (3) high SOL ion temperature at the midplane.

In this study Y_c is varied from 0.4 to 1.4, and over this range the resulting core carbon concentration is virtually unaffected. Since the presence of carbon affects the UEDGE solution, ion fluxes and incident energies are also affected by a change in the multiplier, and the net wall carbon flux does not change proportionally. While Y_c was varied by a factor of 3.5, the carbon source from the wall and divertor plates changed by a factor of 2.4, from 5 to 12×10^{21} C/s. Fig. 2 shows the average core carbon concentration as a function of the carbon source from the wall and divertor plates.

The general flow pattern of carbon through the near SOL is illustrated by the white arrows in Fig. 1. The carbon flows into the near SOL near the separatrix from both divertors, then flows radially outward into the far SOL. In the far SOL, the carbon flows mostly to the inner divertor. Some of the details of this flow are discussed below.

There is a change in divertor conditions and, therefore, divertor screening in these cases. The density of carbon along a flux tube just outside the separatrix ($\psi_{norm} = 1.0046$) as a function of the poloidal length away from the outer divertor plate is shown in Fig. 3. The shape of these curves is similar to that predicted by Stangeby and Elder [2] with a peak near the outer plate, followed by a region of depletion due to the relatively strong frictional force near the plate and a region of growth toward the midplane due to the strong ∇T_i force in this region. These cases do not meet the criterion given by Stangeby and Elder for good screening, i.e., $n_c(\text{valley})/n_c(\text{peak}) < 0.1$.

The change in divertor screening does not completely account for the lack of variation of the core carbon concentration. The flux of carbon escaping the divertor and fueling the near SOL does vary significantly with the carbon source. Fig. 4 shows the flux of carbon entering the SOL from the two divertor plates for the case of $Y_c = 0.7$ as a function of ψ_{norm}. In the region near the separatrix from $1.0 < \psi_{norm} < 1.015$, the carbon flows into the SOL from both divertor legs, whereas the region from $\psi_{norm} = 1.015$ to the UEDGE boundary has very weak flow in the outer divertor and strong flow of carbon back to the divertor on the inner leg. The carbon fueling of the near SOL from the divertor legs is calculated as the total carbon flux through the surfaces defined poloidally by the X-point and radially as $1.0 < \psi_{norm} < 1.015$ on both inner and outer legs. This flux is found to balance the outward radial flux of carbon integrated around the SOL portion of the 1.015 flux surface. This fueling flux is plotted as a function of

Table 3
Divertor plasma parameters from the UEDGE solutions

	Inner plate	Outer plate
Max T_e (eV)	1.31–1.35	18–57
Max n_e (10^{20} m^{-3})	1.84–2.38	7.5–10.8
Max T_i (eV)	1.52–1.56	8.3–12.2

Table 2
Outboard midplane plasma parameters from the UEDGE model of an ELMing H-mode discharge[a]

Outboard midplane	Inner boundary	Separatrix	Outer boundary
ψ_{norm}	0.96	0.9992	1.08
T_i (eV)	1118–1125	488–509	83–101
T_e (eV)	893–906	196–205	25–26
n_e (10^{19} m^{-3})	3.77–3.79	2.67–2.73	0.84–1.08
n_i (10^{19} m^{-3})	3.35	2.32–2.34	0.75–0.82
n_{C+6} (10^{17} m^{-3})	6.66–7.02	5.03–5.69	0.95–2.44

[a] The range shows the variation in each parameter as the sputtering multiplier was scanned.

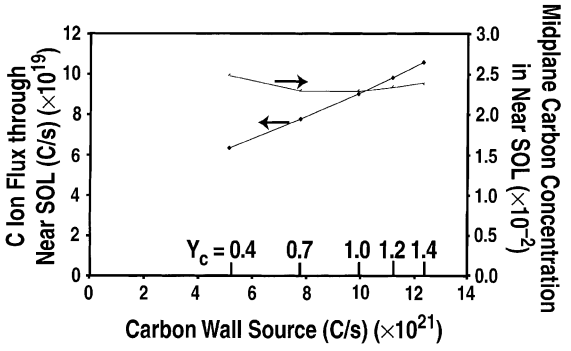

Fig. 2. Midplane carbon concentration in the near SOL and carbon flux through the SOL as a function of the total carbon source from the wall and divertor plates. The values of the sputtering multiplier, Y_c, used in the code are shown along the horizontal axis.

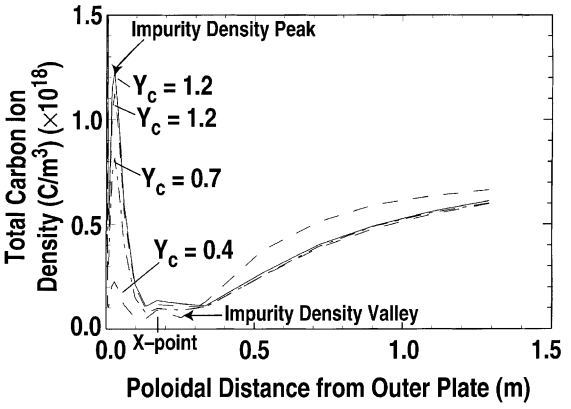

Fig. 3. Carbon ion density as a function of the poloidal distance from the outer strike plate along a flux tube at $\psi_{norm} = 1.0046$.

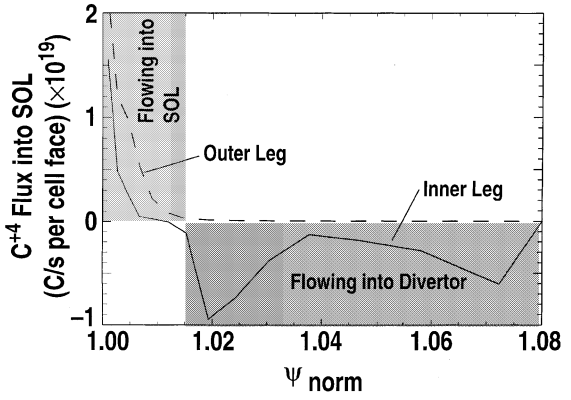

Fig. 4. C^{+4} flow at the interface between the divertors and SOL for both inner and outer legs for the case $Y_c = 0.7$. Positive is toward the SOL for both legs.

carbon source in Fig. 2 and is seen to increase significantly as the carbon source increases.

In order for the midplane carbon density to remain constant while the carbon flux through the near SOL is changing, the radial carbon flux from the near to far SOL must change, as stated above. Since the radial carbon flux is purely diffusive, and the cross field diffusion coefficient was held constant in this study, this implies a change in the radial gradient of carbon. The radial profiles of carbon density at the outboard midplane are shown in Fig. 5. As can be seen, the density of carbon in the far SOL rises as the wall source decreases and the radial gradient decreases. In these cases, a boundary condition of zero carbon ion flux is set at the outer wall, so carbon ions must be transported back to the plate. As seen from Fig. 4, the carbon ions in the far SOL flow to the inner divertor in these cases. Fig. 6 shows that the D^+ flow velocity in the far SOL along the inner wall and to the inner divertor is dropping significantly as the carbon source is decreased. The frictional drag on the carbon ions is also reduced and the flow velocity of the carbon is reduced as shown in Fig. 7. This reduced flow velocity is consistent with the increased carbon density at lower carbon source.

As a check that the zero flux outer boundary condition imposed on these solutions is not strongly influencing the core carbon concentration, a case was run with a different boundary condition, i.e., fixed density for the C^{+6}, C^{+5}, and C^{+4} ionization states at the outer boundary. The case with $Y_c = 0.7$ was used as the starting point. The total density of the three highest ionization states of carbon at the wall was reduced to about 40% of the original value. The midplane carbon concentration at the separatrix, 0.023, was unchanged. A further check was done by increasing the Y_c to 0.8

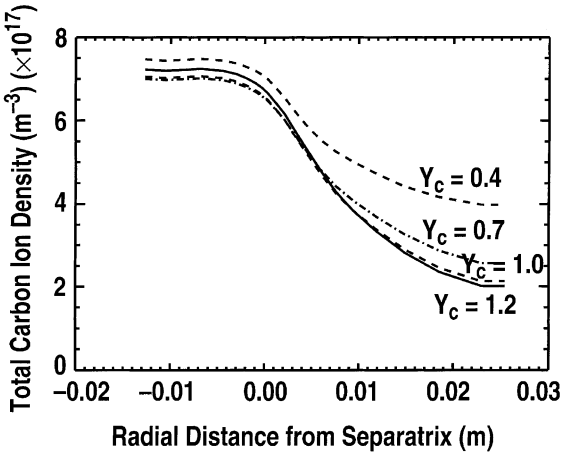

Fig. 5. Total carbon ion density as a function of radial distance from the separatrix at the outboard midplane for four carbon source rates.

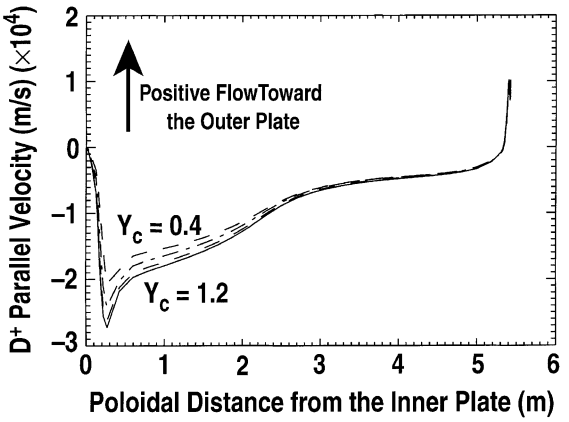

Fig. 6. D^+ parallel flow in the far SOL at $\psi_{norm} = 1.047$ as a function of the poloidal distance from the inner plate for four values of carbon source. Positive flow is toward the outer plate, negative toward the inner.

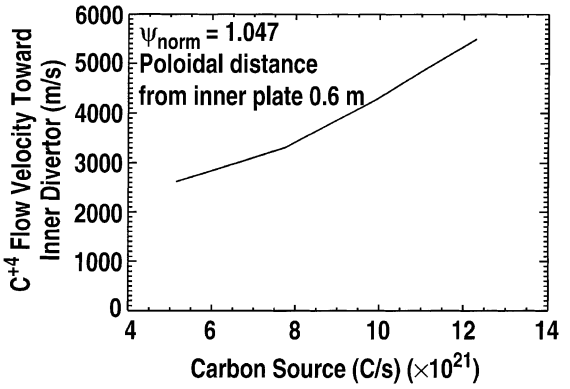

Fig. 7. The flow velocity of C^{+4} ions toward the inner divertor in the far SOL at $\psi_{norm} = 1.047$ and a poloidal distance of 0.6 m from the inner plate are shown as a function of the carbon source as the sputtering multiplier was scanned from 0.4 to 1.4.

with the fixed density boundary condition. The midplane carbon concentration remained at 0.023.

4. Discussion and acknowledgements

The remarkable result that the divertor carbon source on DIII-D has decreased by about a factor of four over the past several years, yet core carbon concentration in typical ELMing H-mode discharges has remained approximately constant [1] is seen to be consistent with UEDGE modeling. These results indicate that attention to SOL transport is at least as important to the control of core impurity contamination as the reduction of the direct wall source. Examination of the carbon flows in these solutions suggests that changes in divertor screening are only partially responsible for the modeling result. Carbon transport in the far SOL is also seen to be important to the overall flow of carbon through the SOL.

Many aspects of the UEDGE fluid model are approximations to the tokamak transport and boundary conditions and may not accurately represent the real plasma. One such example for the UEDGE model is the source of carbon from the main chamber wall, which probably arises from charge exchange neutral sputtering. The main chamber wall neutral sources are not well modeled by UEDGE and neither is the charge exchange sputtering. These studies demonstrate that the divertor can be a very significant source of carbon to the core plasma, but should not be construed to imply that the main chamber wall does not play a role. Additionally, the main chamber wall boundary conditions imposed in these solutions are also in some question and more work is needed in this area.

The modeling and the experimental database are from the open lower divertor configuration in DIII-D. Significant changes in the far SOL can be expected now that strong baffling and divertor pumping are being applied in DIII-D. Modeling of SOL flows will serve as a guide for experimental efforts to control carbon contamination of the core plasma.

This work was supported by the US Department of Energy under Contract Nos. DE-AC03-99ER54463, W-7405-ENG-48, DE-AC05-00OR22725 and Grant No. DE-FG03-95ER54294.

References

[1] D.G. Whyte et al., in: 14th International Conference on Plasma Surface Interactions, 22–26 May, Rosenheim, Germany, 2000.
[2] P.C. Stangeby, J.D. Elder, Nucl. Fus. 35 (1995) 1391 1995
[3] J. Neuhauser, W. Schneider, R. Wunderlich, K. Lackner, Nucl. Fus. 24 (1984) 39.
[4] S.I. Krasheninnikov et al., Nucl. Fus. 31 (1991) 1455.
[5] T.D. Rognlien, J.L. Milovich, M.E. Rensink, G.D. Porter, J. Nucl. Mater. 196–198 (1992) 347.
[6] G.R. Smith, P.N. Brown, R.B. Campbell et al., J. Nucl. Mater. 220–222 (1995) 1024.
[7] L. Lao et al., Nucl. Fus. 30 (1990) 1035.
[8] S.I. Braginskii, in: M.A. Leontovich (Ed.), Review of Plasma Physics, vol. 1, Consultants Bureau, New York, 1965, p. 205.
[9] F. Wising, D.A. Knoll, S. Krasheninnikov, T.D. Rognlien, Contr. Plasma Phys. 36 (1996) 309.
[10] J.W. Davis, A.A. Haasz, J. Nucl. Mater. 241–243 (1997) 37.
[11] W. Eckstein, C. Garcia-Rosales, J. Roth, W. Ottenberger, IPP 9/82, February 1993, Max Planck Institut.
[12] K. Behringer, JET report R(87)08, 1987.